

# INFLUENCING FACTORS ON THE DIELECTRIC BREAKDOWN STRENGTH IN F-GAS FREE HIGH-VOLTAGE SWITCHGEAR

S. GOSSMANN<sup>a,\*</sup>, B. LUTZ<sup>b</sup>, P. G. NIKOLIC<sup>a</sup>

<sup>a</sup> Siemens AG, Corporate Technology, Günther-Scharowsky-Str.1, 91058 Erlangen, Germany

<sup>b</sup> Siemens AG, Energy Management, Nonnendammallee 104, 13629 Berlin, Germany

\* svetlana.gossmann@siemens.com

**Abstract.** After being in the focus of sciences' and industry's research and development activities for many years, the investigation of possible SF<sub>6</sub> gas-alternatives has been even more intensified after the revision of the European regulation on fluorinated gases in 2014. In this contribution the influencing factors on the dielectric breakdown of clean air are investigated for weak inhomogeneous field and gas pressures up to 10 bar. Modelling approaches and experimental data are compared.

**Keywords:** F-gas free switchgear, dielectric breakdown, clean air, surface roughness.

## 1. INTRODUCTION

Nowadays SF<sub>6</sub> (sulphur hexafluoride) is the state-of-the-art insulating and arc quenching medium used in gas-insulated switchgear (GIS), enabling safe current interruption and high dielectric strength. At the same time, if released to the environment, SF<sub>6</sub> is a strong greenhouse gas with a global warming potential of 22800 CO<sub>2</sub> (carbon dioxide) mass equivalents [1–3].

After being in the focus of sciences' and industry's research and development activities for many years, the investigation of possible SF<sub>6</sub> gas-alternatives has been even more intensified after the revision of the European regulation on fluorinated gases in 2014. An assessment of the physical properties of gas-alternatives currently under discussion shows, that the design of future switchgear with SF<sub>6</sub> gas-alternatives requires a detailed consideration of the gas and material properties. In this context it is also expected that a significant change of the design criteria, used for SF<sub>6</sub> switchgear for the last decades, could be necessary. Thus a detailed understanding of the underlying physical processes and breakdown mechanisms as well as of influencing factors on these is necessary.

These influencing factors (e.g. surface roughness, gas pressure etc.) are investigated for clean air in this contribution focussing on weak inhomogeneous field and gas pressures up to 10 bar. Based on these investigations modelling approaches for different effects on the dielectric strength (e.g. influence of protrusion shape and dimensions) of clean air (80 % nitrogen, 20 % oxygen) are analyzed and compared. The investigations are supported by experimental results.

## 2. BASIC THEORY OF STREAMER-DISCHARGE

In this contribution the streamer breakdown mechanism in clean air is investigated. The streamer discharge is driven by impact-ionization and photon emission processes. If electrodes have the same roughness

and are made from the same material, the positive streamer is more critical for the dielectric breakdown. If the avalanche reaches its critical size, a significant field increase occurs in front of the avalanche head and at the avalanche tail. Because of this distortion of the electric field by space-charges, photons are emitted from the avalanche head and in the region behind the avalanche tail. New avalanches are initiated, because the electric field there exceeds the critical electric field, at which the ionization coefficient is greater than the attachment coefficient. In Fig. 1 the development of a positive streamer discharge is depicted [4]. An area with active ionization is located round the head of the streamer with positive charge. In the reduced field area photoelectrons induce new electron avalanches, which develop concentrically toward the streamer head. The large number of electrons entering the streamer head neutralizes the positive space-charge at this location. However, during their development a new center with positive space-charge is formed, which virtually shifts the anode towards the cathode.

The ignition condition for the streamer is fulfilled, if the critical number of free moving charge carriers has reached a number of  $N_{cr} = 10^6 \dots 10^8$  [4]:

$$\int_0^{z_{cr}} \alpha_{eff} dz = \ln N_{cr} \quad (1)$$

where  $\alpha_{eff}$  is the effective ionization coefficient as a function of reduced electric field  $\frac{E}{p}$  and  $z_{cr}$  is the distance ahead the surface, where  $\alpha_{eff} > 0$ .

## 3. ANALYTICAL AND SEMI-EMPIRICAL APPROACHES FOR MODELLING

The quality of surface finish of a metal depends not only upon the material itself but also upon the manufacturing and machining process, respectively. The approach, how to consider the surface roughness and protrusion dimensions, plays an important role for the

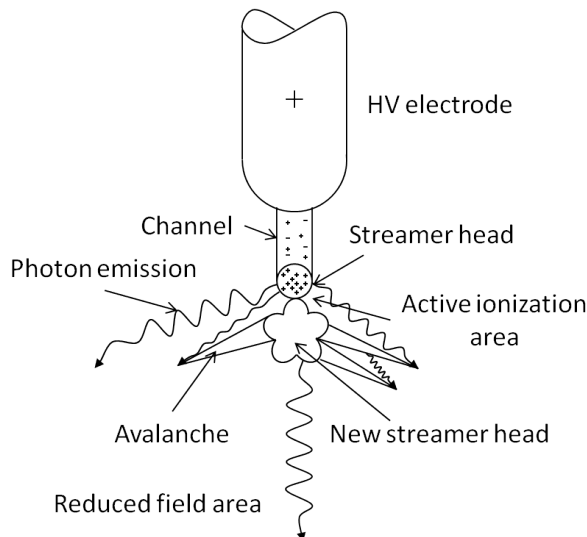


Figure 1. Development of the positive streamer discharge [4]

modeling of the streamer formation. There are different methods, how to implement the surface roughness in the modeling, e.g. fractal theory [5], multi-ridge model [6], calculation of enhancement factor [7–9] and the electric field strength along the axis [9–12].

In the breakdown model used in the context of this contribution, the local field enhancement is emulated by a single idealized protrusion in the form of a prolate semi-ellipsoid evolving from a perfectly smooth conductor. The electric field strength  $E(z)$  normal to the middle of the tip of the protrusion is described by expression [10]:

$$E(z) = E_0 \left[ 1 + \frac{2h \left( \frac{zH}{z^2 - H^2} \right) - \frac{1}{2} \ln \left( \frac{z+H}{z-H} \right)}{h \ln \left( \frac{h+H}{h-H} \right) - 2H} \right], \quad (2)$$

where  $E_0$  is the electric field strength for a perfectly smooth conductor; the protrusion in the form of semi-ellipsoid is characterized by its height  $h$  and half-width  $r$  with  $H = \sqrt{h^2 - r^2}$ . In order to compare different approaches for emulating the electric field strength along the axis, three approaches, Zhirnov [11] (cf. (3)), Jaeger [9] (cf. (4)) and a breakdown model using (2), with the same electric field enhancement factor  $\beta$  are taken into account for a plane-plane set-up with a semi-ellipsoidal protrusion with tip radius  $r_c$  at the high voltage electrode (cf. Fig. 2):

$$E(z) = E_0 \left[ \frac{\beta r_c^2}{(r_c + z)^2} + 1 \right], \quad (3)$$

$$E(z) = E_0 \left[ 1 + \frac{r_c^2}{(z + r_c)^2} \right], \quad (4)$$

For the validation purposes a Finite Element Modeling (FEM) is additionally performed for this plane-plane set-up, considering the same protrusion dimensions as for the analytical approaches.

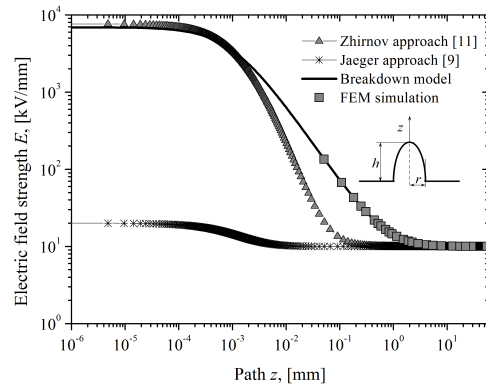


Figure 2. Electric field strength calculated for plane-plane geometry with semi-ellipsoidal protrusion with  $h = 5$  mm and  $r = 0.1$  mm, voltage difference of 600 V and distance between electrodes of 60 mm.

From the results given in Fig. 2 it is observed, that the analytical expression (2) used in the breakdown model yields good agreement with the simulation data for semi-ellipsoidal protrusion. FEM simulations are also performed for a plane-plane set-up with conical protrusion. Since the model used in the context of this contribution has the prolate semi-ellipsoidal form of protrusion, the same height and tip radius are taken for an additional comparison with FEM simulation for a conical protrusion. Both, simulation and modeling results using (2) are found to be in good agreement. Therefore, for the further breakdown analysis only the proposed form of protrusion, prolate semi-ellipsoid, is used.

#### 4. EXPERIMENTAL APPROACH

Set-ups representing typical GIS arrangements were defined for dielectric breakdown tests. The following requirements had to be fulfilled by the model arrangements:

- Field utilization factor  $\eta = E_{\text{average}}/E_{\text{maximum}}$  comparable to typical GIS arrangements
- Surface quality comparable to GIS conditions
- Same electrode materials as in GIS

The distinction between small (i.e. sphere-plane) and big surfaces (i.e. coaxial cylinder) was adopted in order to simulate parts of GIS with smaller and bigger surface area. The model arrangements are shown in Figure 3 where the field utilization factors  $\eta$  of the arrangements are indicated as well.

A variety of different parameters were investigated by high voltage breakdown tests like gas humidity, or the test method [13]. The influence of three parameters, i.e. voltage type, gas pressure and surface roughness, are highlighted in this paper.

According to IEC 62271-1, high dielectric breakdown strength against impulse and AC voltages is required for reliable operation of GIS. Here,  $1.2 \mu\text{s} / 50 \mu\text{s}$

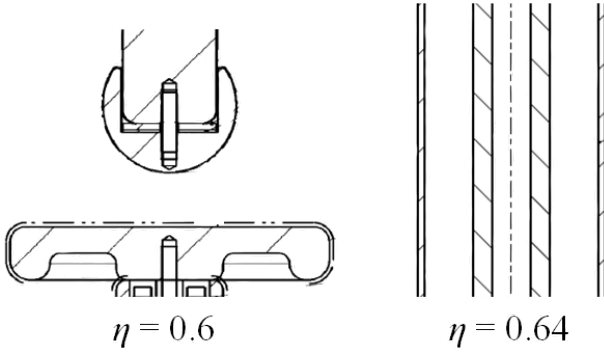


Figure 3. Sphere-plane (left) and coaxial cylinder (right) set-ups for breakdown experiments.

lightning impulse and 50 Hz sinusoidal AC voltage were applied. The up-and-down method [4] was applied to evaluate the breakdown voltage limit values. The choice of gas pressure within a range of 4 bar to 9 bar (absolute value) is important for proper GIS design influencing e.g. size and weight of compartments. Finally, the machining of surfaces influences manufacturing and costs of GIS so that proper surface roughness has to be carefully defined. Here, aluminium electrode surface profiles with mean roughness height of surface profile ranging from 1  $\mu\text{m}$  to 63  $\mu\text{m}$  were evaluated. The experimental results are shown in section 5.

## 5. DISCUSSION OF MODELING AND EXPERIMENTAL RESULTS

The rough surface has a negative influence on the dielectric strength, especially with increasing gas pressure. These effects were previously investigated experimentally [14, 15] and some empirical models were developed [16]. In such models the influence of the electrode protrusion on the dielectric strength is represented by a roughness factor, which is a function of the gas pressure and the protrusion tip radius. It was found that this roughness factor does not depend on the type of applied test voltage (i.e. alternating current (AC) voltage or lightning impulse (LI) voltage) [17]. For this approach measurements with electrodes with varying surface roughness at different gas pressures are needed. In contrast to this, the streamer model for the breakdown analysis used in the context of this contribution applies the parameters for emulating the same surface roughness for different pressures.

In Fig. 4 the experimental results for the coaxial cylinder set-up with polished surface are compared with the modeling results, obtained for the critical charge carrier number  $N_{cr} = 10^8$  as ignition condition [4]. By this approach with constant critical charge carrier number and varying protrusion dimensions, only rough agreement between experimental and modeling data is observed.

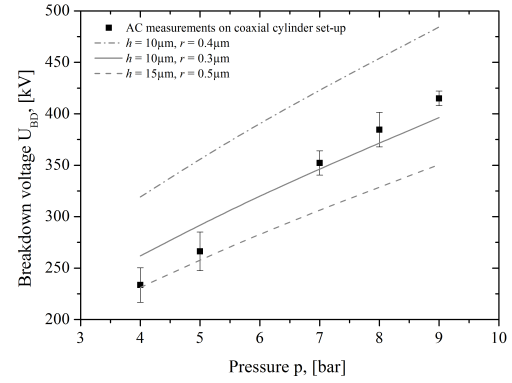


Figure 4. Comparison of experimental and modeling results for critical carrier number of  $N_{cr} = 10^8$ .

Next to the surface roughness the streamer breakdown mechanism significantly depends on the gas pressure. The streamer head dimension as well as avalanche length decrease with increase of pressure. The space-charge field  $E_r$  at the head of the avalanche is also a function of air pressure  $p$ . If avalanche has travelled a distance  $z$  in a non-uniform field, the space-charge field is given by [18]:

$$E_r = 5.27 * 10^{-7} \frac{\alpha_z \exp(\int_0^z \alpha dz)}{\sqrt{\frac{z}{p}}}, \quad (5)$$

where  $\alpha_z$  is the value of effective ionization coefficient,  $\alpha$  corresponding to the external field at the head of the avalanche.

For this reason, in the model used in the context of this contribution, the logarithm of critical number of charge carriers  $\ln N_{cr}$  is taken as a function of pressure, namely  $\sqrt{p}$ . The breakdown analysis utilizing the proposed model is performed for both, sphere-plate and coaxial cylinder set-ups (cf. Fig. 5). Thereby the sphere-plate is stressed by positive LI voltage 1.2  $\mu\text{s}$  / 50  $\mu\text{s}$ , whereas for the coaxial cylinder geometry AC test voltage is applied. For modeling the LI breakdown voltage a constant ratio between AC and LI breakdown voltages is assumed (cf. [19]). In addition the model is calibrated with the measured breakdown voltage at a pressure of  $p = 4$  bar to yield suitable assumptions for the protrusion dimensions in comparison to the given surface roughness of the electrodes. Nevertheless in future investigations also the influence of multiple protrusions with varying dimensions occurring on one electrode surface and their influence on the breakdown process and modeling should be considered. In addition statistical delay times of ignition and spark formation as well as the modeling of the breakdown process in (strongly) non-uniform electric fields will be considered in future development steps of the model and further experimental investigations. Applying the approach described above, the prediction of breakdown voltages for pressure values

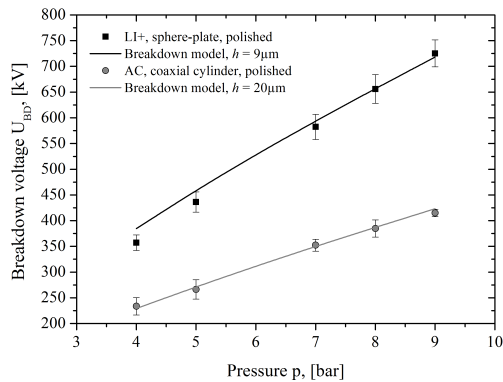


Figure 5. Comparison of experimental and modeling results for  $\ln N_{cr}$  as a function of pressure  $\sqrt{p}$ .

of  $p > 4$  bar is possible and for both set-ups the experimental and modeling results are in good agreement. It is observed, that the results indicate a slightly higher surface roughness for the coaxial cylinders than for the sphere-plate arrangement. For sphere-plate set-up, protrusion with the height  $h = 9 \mu\text{m}$  located at the surface of the sphere needs to be assumed while a protrusion with  $h = 20 \mu\text{m}$  is modeled at the surface of the inner cylinder. Both assumptions are in the expected range for the surface roughness of polished surfaces.

## 6. CONCLUSION

The model described in this contribution is developed for the breakdown analysis in clean air at different pressures taken into account real surface roughness of metal electrodes. The logarithm of the critical number of charge carriers is taken as a function of pressure. For both sphere-plate and coaxial cylinder set-ups, stressed by positive LI and AC voltages, the experimental and modeling results are found to be in good agreement.

Based on the simulation model and experimental results, new and reliable Clean Air GIS design up to 145 kV has been developed [13].

## Acknowledgements

The authors would like to thank A. Geisler for his support with the model development as well as W. Hartmann and T. Hammer for the fruitful discussions.

## References

- [1] UFCCC. *Kyoto Protocol to the united nations framework convention on climate change*. United Nations Framework Convention on Climate Change, 1997.
- [2] D. Gautschi and K. Pohlink. Ist SF<sub>6</sub> in Hochspannungsschaltanlagen ersetzbar? - Neue Forschungsarbeiten bringen ermutigende Resultate. *Bulletin Electrosuisse und Verband Schweizerischer Elektrizitätsunternehmen (VSE)*, 105(12):43–46, 2014.
- [3] B. Lutz et al. Alternativen zu SF<sub>6</sub> - Aktueller Stand und klimaneutrale Auswege. In *Fachtagung Hochspannungs-Schaltanlagen: Anwendungen, Betrieb und Erfahrungen*, Darmstadt, 2016.
- [4] M. Beyer et al. *Hochspannungstechnik*. Springer-Verlag, 1986.
- [5] Y. Zhang et al. Study of Microscopic electric Field on contact Surface in Vacuum Interrupters based on Fractal Theory. *ISDEIV*, pages 29–32, 2016. doi:10.1109/DEIV.2016.7748667.
- [6] R. Li and Y. Qiu. A new multi-ridge model for electrode surface roughness effect in SF<sub>6</sub>. In *Proc. 2nd Int. Conf. Properties and Applications of Dielectric Materials*, pages 105–108, 1988. doi:10.1109/ICPADM.1988.38344.
- [7] H.G. Kosmahl. Analytic Evaluation of Field Emission Enhancement Factors for Ellipsoidal Cones and Elliptic Cross-Section Wedges. *IEEE Transactions on Electron Devices*, 38(6):1534–1537, 1991. doi:10.1109/16.81650.
- [8] C. J. Edgcombe and U. Valdré. Microscopy and computational modelling to elucidate the enhancement factor for field electron emitters. *Journal of Microscopy*, 203(2):188–194, 2001. doi:10.1046/j.1365-2818.2001.00890.x.
- [9] D. L. Jaeger et al. Local electrostatic effects of surface structure on field emission. *Journal of Applied Physics*, 93(1):691–697, 2003. doi:10.1063/1.1526934.
- [10] V.G. Agapov and M.V. Sokolova. The Influence of Electrode Surface Microwhiskers on a Breakdown Voltage of a Pressurized Gas. In *International High Voltage Symposium*, pages 395–398, Zurich, 1975.
- [11] V.V. Zhirnov. On the Cold Emission Mechanism of Diamond Coated Tips. *Journal de Physique*, 6(5):107–112, 1996. doi:10.1051/jp4:1996517.
- [12] A. Galdetskiy. Field Enhancement in some Field Emission Structures and Ion Bombardment Suppression by Applied rf Voltage. In *Technical Digest of IVMC*, pages 598–601, 1997. doi:10.1109/IVMC.1997.627658.
- [13] N. Presser et al. Advanced insulation and switching concepts for next generation High Voltage Substations. In *paper B-108*, Cigré Paris, 2016.
- [14] M. Rossner and A. Hopf. Elektrische Festigkeit von alternativen Isoliergasen bei hohem Druck. *PESS*, page P01.6.
- [15] M. Rossner et al. Dielectric Strength of Alternative Insulation Gases at High Pressure in the Inhomogeneous Electric Field. In *EIC*, pages 369–374, 2015. doi:10.1109/ICACACT.2014.7223618.
- [16] R. Arora and W. Mosch. *High Voltage and Electrical Insulation Engineering*. Wiley-IEEE Press, 2011.
- [17] W. Mosch and W. Hauschild. *Hochspannungsisolierungen mit Schwefelhexafluorid*. VEB Technik Verlag, 1979.
- [18] J.M. Meek and J.D. Craggs. *Electrical breakdown of gases*. Oxford University Press, 1953.
- [19] N. Koshino et al. Partial discharge and breakdown characteristics of CO<sub>2</sub>-based gas mixtures as SF<sub>6</sub> substitutes. In *Gaseous Dielectrics X*, chapter 5, pages 217–222. Springer US, 2004. doi:10.1007/978-1-4419-8979-6\_30.